PHYSICAL REVIEW B VOLUME 23, NUMBER 6 15 MARCH 1981

Theory of radiative recombination by diffusion and tunneling in amorphous Si:H

K. M. Hong and J. Noolandi
Xerox Research Center of Canada, Mississauga, Ontario L5L 1J9, Canada

R. A. Street
Xerox Palo Alto Research Center, Palo Alto, California 94304

(Received 12 May 1980)

A theory for geminate electron-hole recombination in amorphous semiconductors is given, which includes the effects of both diffusion and tunneling. The exact solution of the model is obtained neglecting the Coulomb interaction, which is included later in the prescribed diffusion approximation. It is shown that any combination of diffusion and tunneling will lead to a $t^{-3/2}$ long-time behavior for the reaction rate. The model is used to carry out an analysis of the photoluminescence decay in plasma-deposited amorphous Si:H as a function of temperature. The $t^{-3/2}$ long-time decay is observed at intermediate temperatures ($T \sim 150$ K), and the calculated luminescence quenching is in good agreement with experiment. The initial thermalized pair distribution function of electron-hole separations obtained from the low-temperature ($T = 8$ K) luminescence data is used to determine the Onsager photogeneration efficiency at room temperature. The calculations are in good agreement with the corresponding quantum efficiency obtained from recent xerographic measurements on the same material.

I. INTRODUCTION

Efficient photoluminescence has been reported in hydrogenated amorphous silicon prepared with a low defect density.[1,2] Experimental investigations have resulted in a model of a radiative tunneling mechanism in which the electron and hole are localized in band-tail states, separated by a distance of order 50 Å.[3] Studies of the temperature dependence of the luminescence decay have led to a qualitative understanding of the effects of carrier diffusion on the radiative and nonradiative processes in terms of an Onsager model.[4] Recently we have reported the results of a model calculation which provides a more quantitative description of the recombination.[5] In this paper the calculation and the experiments to which they apply are described in detail.

The samples studied here were prepared by plasma deposition of undiluted SiH_4, using low rf power $(1W)^2$. The time-resolved luminescence measurements were performed by a gated photon counting technique, described in detail elsewhere.[3] Pulsed excitation down to 50 nsec was used, the excitation wavelength being 5309 Å. The luminescence decay is found to be independent of excitation intensity until the electron-hole pair density exceeds about 1.5×10^{8} cm^{-3}, beyond which nongeminate recombination becomes important.[3] The current experiments were all carried out at low light intensities so that recombination takes place mainly through geminate pairs.

The calculation is based on the geminate recombination model used to analyze the photoconductivity quantum efficiency of chalcogenide glasses,[6,7] but which now includes thermally activated diffusion and the radiative tunneling mechanism. We show that the calculated decay is in good agreement with experiment and that reasonable values of the diffusion coefficient are obtained. Various other predictions of the calculation are also discussed.

Before describing the calculations we summarize the experimental information upon which the model is based. The model was developed by Tsang and Street,[3] and is supported by other reported data,[8] although previously a different recombination mechanism has been suggested.[9] The principal experimental result is the observation of a broad distribution of decay times extending from 10^{-8} sec to 10^{-2} sec[3]. The decay is interpreted as a tunneling process in which the radiative recombination rate P_r is given by

$$P_r = \omega_0 \exp(-2r/r_0). \tag{1}$$

ω_0 is of order 10^8 sec^{-1} for an allowed transition, r is the electron-hole separation, and r_0 is the effective Bohr radius. The wide range of decay times originates from the initial distribution $f(r)$ of electron-hole separations. From the decay data one can directly obtain $f(r)$ which typically peaks at $\sim 5r_0$.

Tsang and Street also deduce that a geminate recombination model applies at low excitation intensity. At high intensity there is a transition to nongeminate recombination which occurs when the separation between pairs becomes less than the mean value of r. This transition is observed as a change in the recombination kinetics and can be directly observed in the luminescence decay. All the calculations described here refer to the low-intensity geminate regime, to which the data

also apply.

The use of Eq. (1) is based on the assumption that carrier diffusion is negligible and thus the time dependence of $f(r)$ is governed by tunneling recombination alone. Tsang and Street argue that this assumption is valid at low temperature (~10 K), but breaks down as the temperature is raised. Their evidence is that the radiative decay time is observed to decrease by about an order of magnitude between 10 and 80 K. They interpret the change as a decrease in the mean value of r in Eq. (1), originating from the thermally activated diffusion of the electron and hole. The qualitative description which forms the basis of our calculations is the Onsager model in which these temperature ranges are important:

(1) Low temperatures (0–~20 K). Here diffusion is negligible and the time dependence of $f(r)$ is given by tunneling recombination.

(2) Intermediate temperatures (~20–60 K). Diffusion now becomes significant. The average electron-hole separation is much less than the Onsager radius [Eq. (18)] so that the electron and hole diffuse together,[3] increasing the radiative transition rate.

(3) High temperatures ($\geq$ 60 K). The Onsager radius becomes comparable to, or less than, the average electron-hole separation and the thermal energy is sufficient to overcome the Coulomb interaction. The pair separates, giving a nonradiative process which decreases both the observed decay time and the luminescence efficiency.

The transition between regimes (2) and (3) is taken to be the temperature at which the luminescence efficiency begins to decrease. The transition temperature between regimes (1) and (2) is less easy to establish. However, the assumption of no diffusion at 10 K is supported by the small change in the decay time between 10 and 45 K.

Our calculations therefore use the 8-K decay data to establish the initial distribution $f(r)$ of pair separations. We then introduce a diffusion coefficient D as a parameter which determines the additional time dependence of $f(r)$. Since we are assuming a thermally activated D, the temperature dependence of the decay is implicitly contained in this parameter. The diffusion parameter is assumed to be constant for all electronic sites. In effect we are averaging over the energy distribution of band-tail states. This assumption represents a serious departure from the real situation, but is required to give a tractable calculation. The approximation is most serious at fairly low temperatures when diffusion is over a small distance and is largely determined by the local distribution of states. At high temperatures when diffusion is the dominant effect, a unique value of D is a more reasonable assumption. Details of the calculation follow in Secs. II and III, and a discussion of its application to a-Si:H is given in Sec. IV.

II. SOLUTION OF DIFFUSION EQUATION WITH TUNNELING

For the time being we neglect the Coulomb interaction between the electron-hole pair and take into account only tunneling recombination. The probability density $\rho_0(r,t)$ that the pair is separated by a distance r is determined from the Smoluchowski equation[4]

$$\frac{\partial \rho_0}{\partial t} = D\nabla^2 \rho_0 - \omega_0 e^{-2r/r_0}\rho_0, \tag{2}$$

where D is the sum of the diffusion coefficients of the two particles, r_0 is the tunneling length, and ω_0 the tunneling rate.

The solution of Eq. (2) which is of particular interest here is the radially symmetric Green's function $\rho_0(r,t|u)$, corresponding to the initial condition

$$\rho_0(r,0|u) = \delta(r-u)/(4\pi u^2), \tag{3}$$

where u is the initial separation of the pair, and the boundary condition

$$\rho_0(a,t|u) = 0, \tag{4}$$

where the latter equation describes recombination on a perfectly absorbing (black body) sphere of atomic dimensions at the origin with radius $a<r$. It is convenient to derive the solution in terms of eigenfunctions of Eq. (2) of the form

$$\rho_k(r,t) = g_k(r)e^{-k^2 t}, \tag{5}$$

where g_k satisfies

$$\frac{1}{r^2}\frac{d}{dr}\left(r^2\frac{dg_k}{dr}\right) + (\alpha^2 k^2 - \alpha^2 e^{-2r})g_k = 0, \tag{6}$$

with the boundary conditions

$$g_k(a) = 0, \tag{7}$$

k^2 being the eigenvalue. In Eq. (6) we have used r_0 as the unit of length, ω_0^{-1} as the unit of time, and set $\omega_0 r_0^2/D = \alpha^2$.

It is well known that Eq. (6) can be transformed into a Bessel's equation with the change of variable[10]

$$z = \alpha e^{-r}, \tag{8}$$

$$g_k(r) = (1/r)f_k(z), \tag{9}$$

giving

$$z^2\frac{d^2 f_k}{dz^2} + z\frac{df_k}{dz} + (\alpha^2 k^2 - z^2)f_k = 0. \tag{10}$$

The solutions of Eq. (10) are modified Bessel functions with imaginary index, $I_{\pm i\alpha k}(z)$. Using the boundary condition Eq. (7) we obtain

$$g_k(r) = -\frac{1}{r}\,\mathrm{Im}\left(\frac{I_{i\alpha k}(\alpha e^{-r})}{I_{i\alpha k}(\alpha e^{-a})}\right). \tag{11}$$

The functions $g_k(r)$ form an orthogonal and complete set.

It can be verified easily that

$$\int_0^\infty dr\, r^2 g_k(r) g_{k'}(r) = N_k \delta(k-k'), \tag{12}$$

where

$$N_k = \frac{\sinh(\alpha k\pi)}{2\alpha^2 k |I_{i\alpha k}(\alpha e^{-a})|^2}. \tag{13}$$

The completeness property can be demonstrated by solving Eq. (2) using the Laplace transform and verifying that the only singularity of the solution is a simple branch cut along the negative real axis. This is equivalent to the statement that all the eigenvalues are real, positive, and nondegenerate. The time-dependent Green's function, corresponding to the initial condition Eq. (3) can then be easily obtained:

$$\rho_0(r,t|u) = \frac{1}{4\pi}\int_0^\infty dk\, \frac{g_k(r)g_k(u)}{N_k}\, e^{-k^2 t}, \tag{14}$$

contrary to statements in the literature.[10,11]

At this point we are obliged to comment on a previous solution to Eq. (2) given by Berlin,[12] who claims that $f_k(z)$ must be equal to $K_{i\alpha k}(z)$. Berlin's argument is based on an obvious mathematical error, and consequently his conclusion that the eigenvalue spectrum is discrete is incorrect, as is some of the subsequent work based on his results.[13,14] It is clear from our earlier discussion that the eigenvalues have a continuous spectrum.

In the limit $k \to 0$ it can be shown from Eq. (11) that

$$g_k(r) \simeq \frac{\alpha k h(r)}{I_0(\alpha e^{-a})} \quad (k \to 0), \tag{15}$$

where

$$h(r) = \frac{1}{r}\left(K_0(\alpha e^{-r}) - \frac{K_0(\alpha e^{-a})}{I_0(\alpha e^{-a})} I_0(\alpha e^{-r})\right) \tag{16}$$

is the well-known steady-state solution to Eq. (2).[15] When Eq. (15) is used in conjunction with Eq. (14), the following long-time behavior for the Green's function may be established:

$$\rho_0(r,t|u) \simeq \left(\frac{\alpha^2}{4\pi t}\right)^{3/2} h(r)h(u) \quad (t \to \infty), \tag{17}$$

a result which has been reported earlier by Fabrikant and Kotomin.[15] The amplitude of the density distribution function depends on the initial separation u [through $h(u)$], as well as the point of observation r [through $h(r)$].

III. PRESCRIBED DIFFUSION APPROXIMATION

In order to take into account the Coulomb interaction between the electron-hole pair, we modify Eq. (2) to give[7]

$$\frac{\partial \rho}{\partial t} = D\,\mathrm{div}\left(\vec{\nabla}\rho + \frac{r_c \hat{r}}{r^2}\rho\right) - \omega_0 e^{-2r/r_0}\rho, \tag{18}$$

where $r_c = q^2/\epsilon k_B T$ is the Onsager radius, q is the magnitude of the electronic charge, ϵ is the dielectric constant, and $\hat{r}$ is the unit vector. The exact solution to Eq. (18) is not known. However, at low temperatures where the carrier mobilities are small and recombination takes place predominantly by tunneling, the Coulomb term may be regarded as a small perturbation and treated by a variant of the prescribed diffusion approximation (PDA) developed by Mozumder.[16] We also take the limit of a vanishing radius for the perfectly absorbing sphere at the origin, and set $a = 0$. As we have shown earlier,[7] this does not lead to a divergence, and is equivalent to using the Onsager boundary condition at the origin, $\rho(0,t) \neq \infty$. Only pairs which are initially very close are poorly described in this approximation, while the specific details of recombination of the more distant pairs are unimportant in our model. At room temperature, tunneling recombination may be ignored, as shown in Appendix C, and Eq. (18) may be solved exactly. The validity of the PDA in the high-temperature limit is discussed elsewhere.[7]

In the PDA we assume

$$\rho(r,t) = F(t)\rho_0(r,t), \tag{19}$$

where ρ_0 is the solution of Eq. (2). Substituting Eq. (19) into Eq. (18) and integrating over r we get

$$\ln F(t) = -4\pi D r_c \int_0^t dt'\, \frac{\rho_0(0,t')}{\Omega_0(t')}, \tag{20}$$

where $\Omega_0(t)$ is the survival probability in the absence of the Coulomb interaction,

$$\Omega_0(t) = 4\pi \int_0^\infty r^2 dr\, \rho_0(r,t). \tag{21}$$

The corresponding survival probability including the interaction is then given by

$$\Omega(t) = F(t)\Omega_0(t), \tag{22}$$

and the recombination rate is

$$R(t) = -\frac{d\Omega(t)}{dt}. \tag{23}$$

From Eqs. (20) and (22) we find

$$R(t) = F(t)[4\pi D r_c \rho_0(0,t) + R_0(t)], \tag{24}$$

where $R_0(t)$ is the recombination rate due to diffusion and tunneling alone (neglecting the Coulomb interaction):

$$R_0(t) = 4\pi\omega_0 \int_0^\infty r^2 dr\, e^{-2r/r_0} \rho_0(r,t). \tag{25}$$

Now the solution of Eq. (2) corresponding to the initial condition

$$\rho_0(r,0) = f(r) \tag{26}$$

is given by integrating the normalized initial distribution with the Green's function Eq. (13),

$$\rho_0(r,t) = 4\pi \int_0^\infty u^2 du\, f(u)\rho_0(r,t|u)$$

$$= \int_0^\infty dk\, \frac{e^{-k^2 t} g_k(r)}{N_k} \int_0^\infty du\, u^2 f(u) g_k(u), \tag{27}$$

where we have again used r_0 as the unit of length and ω_0^{-1} as the unit of time.

Using the relation

$$g_k(0) = \frac{2\alpha^2 k}{\pi} N_k, \tag{28}$$

we have

$$\rho_0(0,t) = \frac{2\alpha^2}{\pi} \int_0^\infty dk\, k e^{-k^2 t} \int_0^\infty du\, u^2 f(u) g_k(u), \tag{29}$$

while the corresponding reaction rate and survival probability are given by

$$R_0(t) = 4\pi \int_0^\infty \frac{dk e^{-k^2 t}}{N_k} \int_0^\infty dr\, r^2 e^{-2r} g_k(r)$$

$$\times \int_0^\infty du\, u^2 f(u) g_k(u), \tag{30}$$

$$\Omega_0(t) = \Omega_0(\infty) + \int_t^\infty dt' R_0(t')$$

$$= \Omega_0(\infty) + 4\pi \int_0^\infty \frac{dk e^{-k^2 t}}{k^2 N_k} \int_0^\infty dr\, r^2 e^{-2r} g_k(r)$$

$$\times \int_0^\infty du\, u^2 f(u) g_k(u), \tag{31}$$

where

$$\Omega_0(\infty) = 4\pi \int_0^\infty dr\, r f(r) \left(K_0(\alpha e^{-r}) - \frac{K_0(\alpha)}{I_0(\alpha)} I_0(\alpha e^{-r}) \right). \tag{32}$$

Equation (32) is derived in Appendix A. Corrections to Eqs. (30) and (31) due to the Coulomb interaction may be calculated within the PDA by using Eqs. (20), (22), and (24).

IV. APPLICATION TO *a*-Si:H

Figure 1 shows new luminescence decay data for *a*-Si:H at temperatures ranging from 8 to 150 K. The data are slightly different from those reported by Tsang and Street, for two reasons. First, the luminescence is measured at the peak of the spectrum (~1.4 eV at 8 K) rather than 1.3 eV as in Ref. 3. The time-resolved shift of the luminescence spectrum leads to a weak energy dependence of the decay. In particular, the high energy enhances the fast decay components and causes the change in slope below 10^{-5} sec seen in Fig. 1. Second, we have been particularly careful to use a sufficiently low excitation intensity to avoid the transition to nongeminate recombination. This leads to a larger luminescence intensity at very long times than was reported previously. In our theoretical analysis we neglect the small shift of the time-resolved spectra to lower energy, as well as the fast decay components.

The solid line fit to the 8-K data in Fig. 1 is obtained using the expansion

$$4\pi r^2 f(r) = r e^{-r} \sum_{n=1}^{N} B_n \exp(-A_n e^{-r}), \tag{33}$$

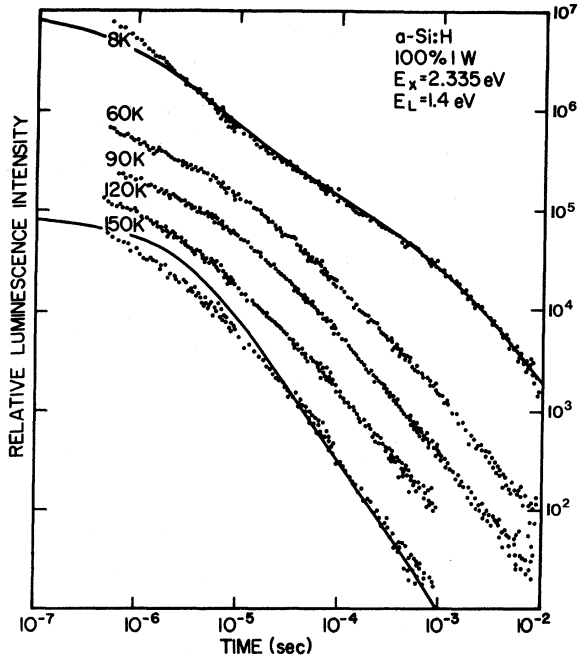

FIG. 1. Log-log plot of photoluminescence decay curves at different temperatures in response to an excitation pulse of short duration. The solid lines show the fit to the theory described in the text. The excitation energy is denoted by E_x, and the luminescence energy E_L.

and the coefficients A_n, B_n are determined by a least-squares fit of the theory to the experimental luminescence intensity given by

$$\log_{10} I(t) = C + \log_{10}[R(t)/R(t_0)], \tag{34}$$

where C is a constant and t_0 corresponds to the time of the first data point. At low temperature the recombination can be reasonably assumed to take place by tunneling only, and in this case Eq. (25) reduces to

$$R_0(t) = 4\pi\omega_0 \int_0^\infty r^2 dr\, e^{-2\pi/r_0} f(r) \exp(-t\omega_0 e^{-2\pi/r_0}), \tag{35}$$

so that Eq. (33) gives

$$R_0(t) = \sum_{n=1}^{N} B_n \int_0^1 du\, u^2 |\ln u| \exp(-A_n u - tu^2). \tag{36}$$

The values of the coefficients up to $N=4$ obtained from a best fit of Eqs. (34) and (36) to the 8-K data are given in Table I. We note that a general numerical evaluation of the recombination rate at higher temperatures is very difficult because of the wide range of integration over k in Eq. (30) and the relatively large values of α (arising from small values of the diffusion coefficient) in the arguments of the Bessel functions. The choice of the functional form for $f(r)$ given by Eq. (33) allows the interior integrals in Eq. (30) to be done analytically (as shown in Appendix B) and greatly simplifies the calculation of the recombination rate.

The shape of the *initial* thermalized distribution of electron-hole pair separations is shown in Fig. 2 and should be compared to the lifetime distribution $G(\tau)$, obtained earlier[3] from an analysis of the data for $T=12$ K, using the expression

$$R(t) = \text{const} \int_0^\infty \frac{d\tau}{\tau} G(\tau) e^{-t/\tau}. \tag{37}$$

Comparing with Eq. (35) in this paper gives

$$4\pi r^2 f(r) = \text{const}\, \tau G(\tau), \tag{38}$$

where $r = (r_0/2)\ln(\omega_0\tau)$ and this relation is valid only when diffusion is negligible.

The thermalization distances shown in Fig. 2 were calculated using $r_0 = 11$ Å, $\omega_0 = 10^8$ sec^{-1}.[3]

TABLE I. Values of parameters for normalized distribution function, Eq. (33).

n	A_n	B_n
1	9.369×10^2	-3.238×10
2	2.226×10^3	1.636×10
3	7.944×10	1.564×10
4	5.903	5.534×10^{-1}

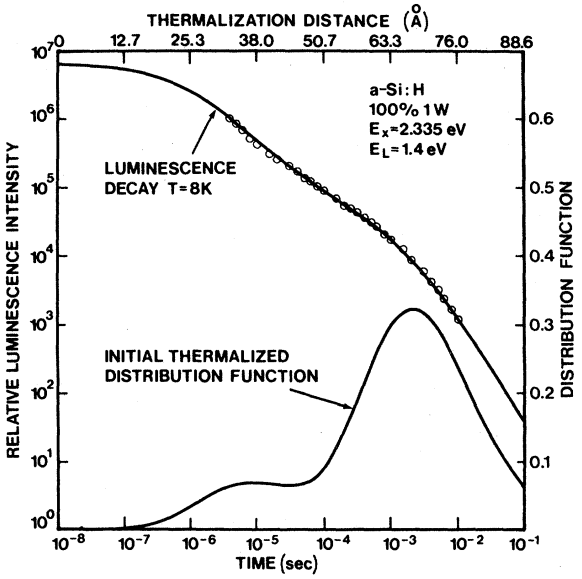

FIG. 2. Initial thermalized distribution function of electron-hole pair separations, obtained from a least-squares fit of Eqs. (34) and (36) to the data shown in the figure. The thermalization distances (upper scale) for the distribution function were calculated using the relation following Eq. (38) in the text and assuming $r_0 = 11$ Å, $\omega_0 = 10^8$ sec^{-1}. As in Fig. 1, E_x denotes the excitation energy, and E_L is the luminescence energy.

The small hump in the distribution function for $t \sim 10^{-5}$ sec shown in Fig. 2 is absent in the earlier analysis. This feature arises from the best fit of our theoretical curve to experimental points which are slightly scattered at short times. Otherwise the distribution functions are very similar, as expected from Eq. (38).

We now assume that the initial distribution function remains unchanged as the temperature is increased, and the change in the luminescence decay is due solely to thermally activated diffusion. Of course when diffusion becomes important the relation Eq. (38) is no longer valid, although it may still be useful to calculate a temperature-dependent lifetime distribution which incorporates the effects of diffusion in some average way.[3] For a fixed initial distribution, the reaction rate at higher temperatures depends on only one parameter, α. The solid-line fit to the 150-K data in Fig. 1 is obtained from the calculation with a value for α of 7 ± 1.

We find that most of the decrease in luminescence intensity at higher temperatures is due to a combination of tunneling and pure diffusion, and the effect of the Coulomb interaction is negligible except for short times (corresponding to small distances). The value of the diffusion coefficient required to fit the data is so small as to practically eliminate the contribution of the Coulomb term

(containing r_c) in Eq. (24). We speculate that the small effect of the Coulomb term may be related to potential fluctuations in the amorphous material, which tend to localize the charge, leading to an effectively reduced Coulomb interaction in our model.

One important general result of the calculation is that in the diffusive regime the decay has a time dependence $t^{-3/2}$ [see Eq. (17)]. Figure 1 shows that the high-temperature data accurately follow this relation, thus providing strong experimental support for the model. The asymptotic curve for the pure tunneling case is reached for longer times than shown in Fig. 2, and the theoretical result is of little value here because it depends on the form of the distribution function outside the interval for which it is accurately known. The small discrepancy between the calculations and the data at short decay times may arise for at least two reasons. One is the presence of a fast component in the decay due to thermalizing carriers which we have not allowed for in the calculation. The second is that our assumption of a single value for the diffusion coefficient is most likely to break down at short times, when the effects of the local distribution of sites is most important. Taking into account these effects, we believe that our results show good agreement between theory and experiment.

Two further checks on the validity of the model can be obtained from our calculations. First, from the value of α we deduce a mobility of 2×10^{-6} cm^2/V sec, using the Einstein relation, and the values of ω_0, r_0 quoted earlier. We anticipate an uncertainty in this value of not more than an order of magnitude, arising mostly from the estimates of ω_0. Thus our results compare reasonably well with the measured electron mobility at $T=150$ K in similar samples of 10^{-5} cm^2/V sec.[17] Second, the temperature dependence of the luminescence intensity can be estimated from the calculation under the assumption that it is represented by the fraction of electron-hole pairs that do not separate. At $T=90$ K we estimate the luminescence quantum efficiency to be 70%, which is in excellent agreement with the observed decrease from the peak value. This result provides independent confirmation of the validity of the model.

Finally we use the initial thermalized distribution function shown in Fig. 2 to estimate the quantum efficiency of photoconductivity at room temperature as a function of the electric field, assuming that all charge carriers which do not recombine can be collected by the electrodes. Of course, we would expect this assumption to be valid only at high electric fields, and in general the observed photogeneration efficiency at low fields would be lower than the theoretical value because of trapping in the bulk. At room temperature the dimensionless parameter $\alpha^2=\omega_0 r_0^2/D$ is very small ($\sim10^{-4}$), and the effect of tunneling can be taken into account in a perturbation calculation, as outlined in Appendix C. The end result is that tunneling is completely negligible at $T=300$ K, and Fig. 3 shows the results of the standard Onsager calculation of the quantum efficiency,[6] except for the fact that we have integrated over the actual distribution function shown in Fig. 2 instead of using the spherically symmetric δ function. The interpolated values of the photogeneration efficiency for a-Se at the same excitation energy are shown by the dotted line, and are obtained from the data in Ref. 6. The curve for a-Si:H is higher than reported previously because earlier[18] we used an incorrect value for the dielectric constant. The results shown in Fig. 3 were obtained using the correct value, $\epsilon=11.5$.

As usual in the Onsager calculation of the quantum efficiency, we assumed a perfectly absorbing sphere of small radius at the origin of the recombination center. If the electron-hole pair encounters a potential barrier at small separations, it would be more appropriate to assume a partly reflecting boundary condition,[19] and this would increase the calculated quantum efficiency over that shown in Fig. 3. However, in the absence of any microscopic information about the final recombination step, we choose a perfectly absorbing boundary and compute the lower limit to the theoretical quantum efficiency shown in the figure.

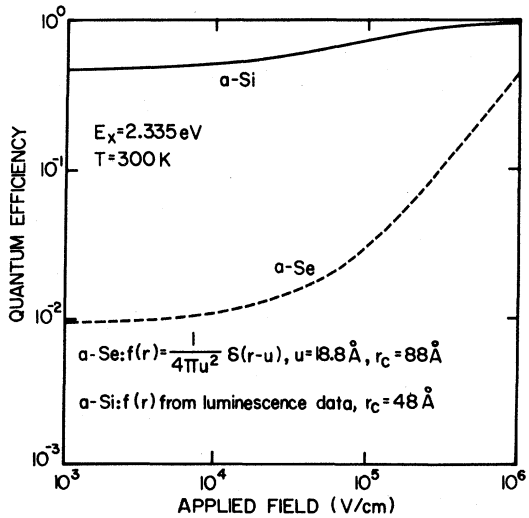

FIG. 3. Calculated quantum efficiency of photoconductivity (charges/photon) for a-Si:H, using the distribution function shown in Fig. 2. The curve for a-Se at the same excitation energy (E_x) is obtained by interpolating the results of Ref. 6.

However, this curve is still expected to be higher than the observed quantum efficiency at low electric fields because of trapping in the bulk, as mentioned earlier.

Recently xerographic discharge measurements have been carried out on samples similar to those used for the photoluminescence measurements.[20] For high electric fields ($E \sim 5\times10^4$ V/cm) the calculations are in excellent agreement with experiment. At lower field strengths, carrier trapping is observed and we will have to wait until a more involved experiment is performed to verify our calculation over the whole field range. Nevertheless the fact that the predicted high quantum efficiencies are observed at high fields adds more support for the geminate recombination model.

V. DISCUSSION AND CONCLUSIONS

Geminate recombination has previously been discussed for chalcogenide glasses. In that case, emphasis has been on the quantum efficiency of photoconductivity, which is given by the fraction of pairs that do not undergo geminate recombination. The validity of the model for a-Si:H suggests widespread applicability to amorphous semiconductors. The same $t^{-3/2}$ decay is observed in amorphous Si:O for a wide range of compositions,[21] and the luminescence decay in a-As_2S_3 also extends over many decades in time with a $t^{-3/2}$ asymptotic behavior.[22] These results are perhaps not surprising because the model is of particular relevance to systems with a short carrier mean free path. There are, however, differences in the detailed application of the geminate model for chalcogenides and a-Si:H. Chalcogenide glasses are noted for a room-temperature photoconductivity quantum efficiency which depends strongly on both electric field and excitation energy. However, similar effects are much less pronounced in nonchalcogenides. It has been argued that this is due to a different mechanism of geminate recombination. It is assumed that chalcogenides have a very efficient nonradiative recombination mechanism over a wide range of temperature, while in a-Si:H it is much weaker. Our results support this model in that we find at higher temperatures ($T > 150$ K) the diffusion rate is sufficiently large to quench the radiative recombination by tunneling. Thus, unless some other geminate process takes over, we would predict a photoconductivity quantum efficiency close to unity and approximately independent of electric field and excitation energy. However, if the temperature is sufficiently low that the luminescence has high efficiency, we predict that the photoconductivity quantum efficiency will show a strong dependence on electric field and excitation energy. Further experimental investigation of these effects would be very valuable.

In conclusion, we have developed a new model of geminate recombination which includes tunneling and diffusion, and we have discussed photoluminescence and quantum efficiency of photoconductivity measurements which give strong evidence for the applicability of the model to a-Si:H. In addition, we have obtained an estimate of the microscopic mobility which can be related to future time-of-flight experiments. We suggest that the luminescence of chalcogenide glasses can be explained by the same recombination mechanism which takes place in a-Si:H and we note that our model can apply to transitions involving defect states provided that one of the carriers is free to diffuse in band-tail states.

ACKNOWLEDGMENTS

We would like to thank L. Marks for assistance in developing the computer programs used to evaluate the reaction rate and related quantities, and J. Mort for discussions regarding the xerographic discharge measurements.

APPENDIX A: ESCAPE PROBABILITY FOR DIFFUSION AND TUNNELING

The ultimate survival probability for the case of diffusion with tunneling can be determined from the steady-state solution $\rho_0(r|u)$. For the initial condition Eq. (3), the corresponding steady-state equation is (in dimensionless variables)

$$\frac{1}{\alpha^2 r^2}\frac{d}{dr}\left(r^2\frac{d\rho_0}{dr}\right) - e^{-2r}\rho_0 = -\frac{1}{4\pi u^2}\delta(r-u). \quad \text{(A1)}$$

The general solution of the homogeneous part of Eq. (A1) is a linear combination of the functions $r^{-1}K_0(\alpha e^{-r})$ and $r^{-1}I_0(\alpha e^{-r})$. Using the boundary conditions

$$\rho_0(a|u) = \rho_0(\infty|u) = 0, \quad \text{(A2)}$$

$$\rho_0'(u+0|u) - \rho_0'(u-0|u) = -\frac{\alpha^2}{4\pi u^2}, \quad \text{(A3)}$$

the last equation being due to the inhomogeneous source term in Eq. (A1), we obtain the solution

$$\rho_0(r|u) = \frac{\alpha^2}{4\pi r_>} I_0(\alpha e^{-r_>}) h(r_<), \quad \text{(A4)}$$

where

$$r_> = \max(r,u),$$
$$r_< = \min(r,u). \quad \text{(A5)}$$

and $h(r)$ is defined by Eq. (16).

The survival probability or escape rate is then easily obtained as

$$\Omega_0(\infty) = \lim_{r\to\infty}\left(-\frac{4\pi r^2}{\alpha^2}\frac{d}{dr}\rho_0(r|u)\right)$$
$$= h(u). \quad \text{(A6)}$$

Setting $a = 0$ and integrating Eq. (A6) over the initial distribution $f(r)$ then gives Eq. (32).

APPENDIX B: COMPUTATIONAL METHODS

From Eqs. (11), (30), and (31), we see that it is necessary to compute integrals of the form

$$I_1 = \int_0^\infty dr\, r e^{-2r} I_{i\mu}(\alpha e^{-r}) \quad \text{(B1)}$$

and

$$I_2 = \int_0^\infty dr\, e^{-r} \exp(-Ae^{-r}) I_{i\mu}(\alpha e^{-r}), \quad \text{(B2)}$$

where $\mu = \alpha k$.

Using the series expansion for the Bessel function, we find

$$I_1 = \sum_{k=0}^{\infty} \frac{(\alpha/2)^{2k+i\mu}}{k!\Gamma(1+k+i\mu)(2+2k+i\mu)^2}, \quad \text{(B3)}$$

and

$$I_2 = \int_0^1 du\, e^{-Au} I_{i\mu}(\alpha u)$$
$$= \sum_{k=0}^{\infty} \frac{(\alpha/2)^{2k+i\mu}\Gamma(2k+1+i\mu)\gamma^*(2k+1+i\mu, A)}{k!\Gamma(1+k+i\mu)}, \quad \text{(B4)}$$

where $\gamma^*(a,z)$ is the incomplete gamma function[23] which may be generated using the recurrence relation[23]

$$z\Gamma(a+1)\gamma^*(a+1,z) = a\Gamma(a)\gamma^*(a,z) - e^{-z}. \quad \text{(B5)}$$

When $A \gg \alpha$, the upper limit of the integral in Eq. (B4) may be extended to ∞ and in this case we get[24]

$$I_2 = \frac{\exp[-i\mu ch^{-1}(A/\alpha)]}{(A^2-\alpha^2)^{1/2}} \quad (A \gg \alpha). \quad \text{(B6)}$$

For moderate values of μ, Eqs. (B3)–(B6) can be used in the computation. However, when μ is small, the real parts of these integrals dominate and the imaginary parts generated become inaccurate in this case. It is then necessary to compute the imaginary parts of the integrals separately. Thus we also require expressions for the following integrals:

$$J_1 = \int_0^\infty dr\, r e^{-2r} K_{i\mu}(\alpha e^{-r}), \quad \text{(B7)}$$

$$J_2 = \int_0^\infty dr\, e^{-r} \exp(-Ae^{-r}) K_{i\mu}(\alpha e^{-r}). \quad \text{(B8)}$$

Using the integral representation for the Bessel function[23]

$$K_{i\mu}(z) = \int_0^\infty dt (\cos\mu t)\exp(-z\,ch\,t), \quad \text{(B9)}$$

we find[24]

$$J_1 = \int_0^\infty dt \cos\mu t \int_0^1 du\, u|\ln u|\exp(-\alpha u\, ch\, t)$$
$$= \int_0^\infty dt \cos\mu t \frac{\ln(\alpha\, ch\, t) + (\gamma-1) + \exp(-\alpha\, ch\, t) + E_1(\alpha\, ch\, t)}{\alpha^2 ch^2 t}$$
$$= \frac{(\mu\pi/2)[\ln(\alpha/2) - \mathrm{Re}\psi(1+i\mu/2)]}{\alpha^2 sh(\mu\pi/2)} + \frac{1}{\alpha^2}\int_0^\infty dt \frac{\cos\mu t}{ch^2 t}[\exp(-\alpha\, ch\, t) + E_1(\alpha\, ch\, t)], \quad \text{(B10)}$$

where $\psi(z)$ is the digamma function[23] and $E_1(z)$ is the exponential integral. Note that for $\alpha \gg 1$, the remaining integral in Eq. (B10) is negligible compared to the first term:

$$J_1 \simeq \frac{(\mu\pi/2)[\ln(\alpha/2) - \mathrm{Re}\psi(1+i\mu/2)]}{\alpha^2 sh(\mu\pi/2)} \quad (\alpha \gg 1). \quad \text{(B11)}$$

Similarly,

$$J_2 = \int_0^\infty dt \frac{(\cos\mu t)[1-\exp(-A-\alpha\, ch\, t)]}{A+\alpha\, ch\, t}, \quad \text{(B12)}$$

so that for $(A+\alpha) \gg 1$ we have[24]

$$J_2 \simeq \int_0^\infty dt \frac{\cos\mu t}{A+\alpha\, ch\, t}, \quad (A+\alpha \gg 1)$$
$$= \frac{\pi}{(A^2-\alpha^2)^{1/2}} \frac{\sin[\mu ch^{-1}(A/\alpha)]}{sh(\mu\pi)} \quad (A > \alpha)$$
$$= \frac{\pi}{(\alpha^2-A^2)^{1/2}} \frac{\mathrm{sh}[\mu\cos^{-1}(A/\alpha)]}{sh(\mu\pi)} \quad (A < \alpha). \quad \text{(B13)}$$

APPENDIX C: PERTURBATION TREATMENT OF TUNNELING

From the nondimensional form of the modified diffusion equation [cf. Eq. (5)], we see that the

tunneling term is proportional to $\alpha^2=\omega_0 r_0^2/D$. At room temperature, $D\sim 10^{-2}$ cm^2/sec,[25] so that $\alpha^2\sim 10^{-4}$ and hence the tunneling term can be treated as a small perturbation.

The steady-state Smoluchowski equation is

$$\mathrm{div}\vec{j}(\vec{r}) = f(\vec{r}) - \omega_0 e^{-2r/r_0}\rho(\vec{r}), \tag{C1}$$

where

$$\vec{j}(\vec{r}) = -De^{-W}\vec{\nabla}(e^{W}\rho) \tag{C2}$$

is the current density, $f(\vec{r})$ is the normalized initial distribution function which acts as a continuous source term here, and W is the total potential divided by k_BT:

$$W = -\left(\frac{r_c}{r} + \frac{2Fr}{r_c}\cos\theta\right), \tag{C3}$$

where $F=qEr_c/2k_BT$, E is the applied electric field, and θ is the angle between $\vec{r}$ and the field.

Using the perturbation expansion up to order α^2, we obtain

$$\rho(\vec{r}) = \rho_0(\vec{r}) + \rho_1(\vec{r}), \tag{C4}$$

with

$$\mathrm{div}\vec{j}_0(\vec{r}) = f(\vec{r}), \tag{C5}$$

$$\mathrm{div}\vec{j}_1(\vec{r}) = -\omega_0 e^{-2r/r_0}\rho_0(\vec{r}), \tag{C6}$$

where $\vec{j}_0$ and $\vec{j}_1$ are the current densities corresponding to ρ_0 and ρ_1. Equations (C5) and (C6) may be solved by using the Green's function $\rho_0(\vec{r}|\vec{u})$ satisfying

$$\mathrm{div}\vec{j}_0(\vec{r}|\vec{u}) = \delta(\vec{r}-\vec{u}), \tag{C7}$$

which has been obtained by Onsager.[4] Thus we have

$$\rho_0(\vec{r}) = \int d^3u f(\vec{u})\rho_0(\vec{r}|\vec{u}), \tag{C8}$$

$$\rho_1(r) = -\omega_0\int d^3u e^{-2u/r_0}\rho_0(\vec{u})\rho_0(\vec{r}|\vec{u}), \tag{C9}$$

and the escape probability can be written as

$$\Omega = \lim_{s\to\infty}\oiint d\vec{s}\cdot\vec{j}(\vec{r}) = \Omega_0+\Omega_1, \tag{C10}$$

where

$$\Omega_0 = \int d^3u f(\vec{u})\Omega_0(\vec{u}), \tag{C11}$$

$$\Omega_1 = -\omega_0\int d^3u e^{-2u/r_0}\rho_0(\vec{u})\Omega_0(\vec{u}), \tag{C12}$$

and

$$\Omega_0(\vec{u}) = \lim_{s\to\infty}\oiint d\vec{s}\cdot\vec{j}_0(\vec{r}|\vec{u}) = \frac{\exp[-(Fu/r_c)(1+\cos\theta)]}{u}\int_{r_c}^{\infty} dr\exp\left(\frac{-r}{u}\right)I_0\left[\left(4F(1+\cos\theta)\frac{u}{r_c}\right)^{1/2}\right] \tag{C13}$$

is the well-known Onsager escape probability for particles generated at $\vec{u}$, which makes an angle θ with $\vec{E}$.

[1] D. Engemann and R. Fischer, in *Proceedings of the 12th International Conference on the Physics of Semiconductors*, edited by M. H. Pilkuhn (Teubner, Stuttgart, 1974), p. 1042.

[2] R. A. Street, J. C. Knights, and D. K. Biegelsen, Phys. Rev. B 18, 1880 (1978).

[3] C. Tsang and R. A. Street, Phys. Rev. B 19, 3027 (1979).

[4] L. Onsager, J. Chem. Phys. 2, 599 (1934); Phys. Rev. 54, 554 (1938).

[5] J. Noolandi, K. M. Hong, and R. A. Street, Solid State Commun. 34, 45 (1980).

[6] D. M. Pai and R. C. Enck, Phys. Rev. B 11, 5163 (1975).

[7] K. M. Hong and J. Noolandi, J. Chem. Phys. 69, 5026 (1978).

[8] I. G. Austin, T. S. Nashashibi, T. M. Searle, P. G. Le Comber, and W. E. Spear, J. Non-Cryst. Solids 32, 373 (1979).

[9] D. Engemann and R. Fischer, in *Structure and Excitation of Amorphous Solids*, edited by G. Lucovsky and F. L. Galeener (AIP, New York, 1976).

[10] M. J. Pilling and S. A. Rice, J. Chem. Soc. Faraday Trans. 2 71, 1563 (1975).

[11] P. R. Butler and M. J. Pilling, Discuss. Faraday Soc. 63, 38 (1977).

[12] Yu. A. Berlin, Dokl. Akad. Nauk SSSR 223, 1387 (1975).

[13] R. F. Khairutdinov, Khim. Vys. Energ. 10, 556 (1976).

[14] Yu. A. Berlin and R. F. Khairutdinov, Khim. Vys. Energ. 12, 3 (1978).

[15] I. Fabrikant and E. Kotomin, J. Lumin. 9, 502 (1975).

[16] A. Mozumder, J. Chem. Phys. 48, 1659 (1968).

[17] G. Pfister, private communication.

[18] J. Noolandi, K. M. Hong, and R. A. Street, J. Non-Cryst. Solids 35 & 36, 669 (1980).

[19] J. Noolandi and K. M. Hong, J. Chem. Phys. 70, 3230 (1979).

[20] J. Mort, S. Grammatica, J. C. Knights, and R. Lujan, unpublished.

[21]R. A. Street and J. C. Knights, Philos. Mag. B 42, 551 (1980).
[22]G. H. Higashi and M. Kastner, J. Non-Cryst. Solids 35 & 36, 921 (1980).
[23]*Handbook of Mathematical Functions*, edited by M. Abramowitz and J. C. Stegun (Dover, New York, 1965).
[24]I. S. Gradshteyn and I. M. Ryzhik, *Tables of Integrals, Series and Products* (Academic, New York, 1965).
[25]We estimate the diffusion constant at room temperature using the Einstein relation, with the mobility $\mu \sim 0.5$ cm^2/Vsec (G. Pfister, private communication).